Buoyancy-Driven Fluid Migration in Porous Media

Vidar Frette,[1] Jens Feder,[1] Torstein Jøssang,[1] and Paul Meakin[1,2]
[1]*Department of Physics, University of Oslo, Box 1048, Blindern, 0316 Oslo 3, Norway*
[2]*Central Research and Development Department, The duPont Company, Wilmington, Delaware 19880-0356*
(Received 19 December 1991)

The slow upward migration, due to buoyancy, of a nonwetting fluid through a saturated, three-dimensional porous medium has been studied experimentally, and by computer simulations. The height h of the invading fluid structure is proportional to the mass M of the invading fluid. The linear mass density $S=M/h$ is found to scale with the dimensionless Bond number Bo (ratio of buoyancy and capillary forces) as $S=A|\mathrm{Bo}|^{-\alpha}$, with $\alpha=0.72\pm0.06$, consistent with theory and simulations. A noisy behavior in $h(M)$ results from dynamical processes such as snapoffs and bursts.

PACS numbers: 47.55.Mh, 05.40.+j, 47.55.Kf, 64.60.Ak

Slow immiscible fluid-fluid displacement in a porous medium plays a major role in many natural and commercial processes. An important class of examples is the wetting and drying of granular materials such as soils, rocks, ceramic powders, and foods. Another example that provided the initial motivation for the work described in this Letter is the migration of hydrocarbons through water saturated rocks, where they may accumulate beneath a trap to build up an oil reservoir. Fluid-fluid displacement during oil recovery and the penetration of spilled hazardous liquids into the ground are important related processes. The complex (often fractal) patterns [1–4] formed during these processes have been the subject of intense scientific interest during the past decade. The development of a better understanding of these fluid-fluid displacement processes is a challenging scientific problem with a broad range of potential applications.

During slow displacement capillary forces dominate over viscous forces leading to patterns described by the invasion percolation model [5]. However, in most cases there are density differences so that gravity causes hydrostatic pressure gradients [6]. These gradients compete with capiliary forces that are randomly distributed due to the randomness of the porous medium. The competition between these two effects can be expressed in terms of a new characteristic length ξ, in addition to the intrinsic length of the medium (e.g., the grain size). On the other hand, the direct ratio of buoyancy forces to capillary forces is given by the dimensionless Bond number: $\mathrm{Bo}=\Delta\rho g a^2/\gamma$, where $\Delta\rho$ is the difference in density between the fluids, g is the acceleration of gravity, a is a typical pore size, and γ is the fluid-fluid interfacial tension.

Little experimental information on gravity effects is available. If the invading fluid is less dense than the defending fluid and enters from the top ($\mathrm{Bo}>0$), then gravity stabilizes the front and the width of the front has been shown [7] to scale as $\xi\sim\mathrm{Bo}^{-0.57}$ in two-dimensional (2D) experiments and simulations. Clément and coworkers [8] performed three-dimensional (3D) invasion percolation experiments, also with gravity stabilization. However, they used only one value of Bo. The same holds true for 3D displacement experiments analyzed using magnetic resonance tomography by Chen *et al.* [9]. Dembicki and Anderson [10] observed that a fluid driven by buoyancy through a porous medium moved along restricted pathways. The unstable infiltration of a (denser) wetting fluid into a dry porous medium has been studied by Glass, Parlange, and Steenhuis [11].

Here we describe 3D experiments for unstable ($\mathrm{Bo}<0$) migration where Bo was varied systematically by adjusting the density of the migrating fluid. The resulting structures were studied quantitatively and compared to theory and computer simulations. Figure 1 shows typical structures obtained in experiments and simulations at two different values for Bo. We have observed a number of new phenomena caused by the instability of the flow. Quantitatively our main finding is that the linear density $S=M/h$ (structure mass per height) can be expressed as $S=A|\mathrm{Bo}|^{-\alpha}$, where experimentally $\alpha=0.72\pm0.06$, consistent with the value $\alpha\simeq0.70$ from theoretical arguments and from extensive simulations.

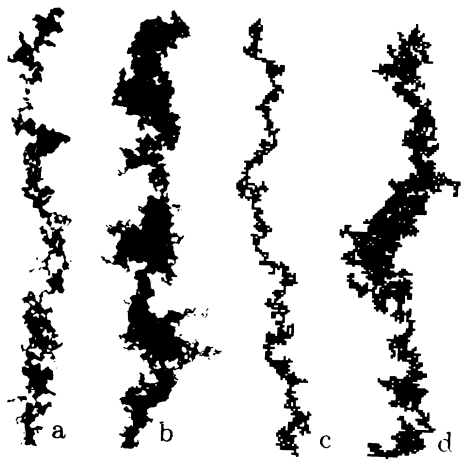

FIG. 1. Photographs of structures obtained during buoyancy-driven fluid migration through a 3D porous medium at (a) $\mathrm{Bo}\simeq-0.40$ and (b) $\mathrm{Bo}\simeq-0.046$. Projections of clusters obtained in computer simulations of 3D invasion percolation with gradients (c) $g=-2.7\times10^{-2}$ and (d) $g=-3.0\times10^{-3}$. The ratio between these gradients was 9 and equal to the ratio of the Bond numbers in (a) and (b).

A modified version of the invasion percolation algorithm was used for the numerical work [5,6]. The invasion percolation model was designed to mimic the displacement of a wetting fluid by a nonwetting fluid (drainage) in the limit of very slow flow, where viscous effects can be ignored so that the process is governed solely by capillary forces. The displacement is assumed to be quasistatic, so that only one new pore is invaded at a time. Each displacement step takes place through the widest pore neck at the fluid-fluid interface, i.e., along the path of least resistance.

The experimental systems were random packings of cylindrical grains (2 mm diameter and 2 mm length) of Röhm Plexiglas Formmasse 7N Glasklar [poly(methylmethacrylate)] (PMMA). The packings were saturated with dibutyl-phthalate, a clear fluid with a viscosity $\mu \simeq 21$ cP and refractive index $n = 1.491$. Since this value matched the refractive index of PMMA, the saturated packings were transparent, and the structure formed by a second fluid invading the medium could be observed directly. The packings were held in a glass container of inner dimensions $18.3 \times 18.3 \times 28.3$ cm^3 (x,y,z) or about $90 \times 90 \times 140$ in terms of the grain size. The porosity was found to be 0.34. Assuming that there were as many pores as grains in these models we determined a characteristic pore volume to be $v = 3.2$ mm^3. As the invading fluid we used solutions of sucrose [(0–60)% by weight] in water, dyed with 1 g negrosin/kg. This fluid was immiscible with dibutyl-phthalate. The density of the dibutyl-phthalate (the wetting fluid) was $\rho = 1.046$ g/cm^3. Equal density of the two fluid phases was obtained for 11.9% sucrose (by weight) in water at room temperature. The interfacial tension was measured to be $\gamma = 13 \pm 1.5$ dyn/cm using a version of the drop weight method [12].

The low (high) concentration solutions were injected from a point source at the bottom (top) of the model, giving rise to unstable structures that evolved upwards (downwards). These two configurations are physically equivalent, and for convenience we refer to all the experiments as buoyancy driven. The invading fluid was injected at a constant rate of 2 ml/h (about 0.17 filled pore/sec). The models were illuminated from the rear and the evolving migration structures were photographed in two projections (see Fig. 1). A typical plot of structure height as a function of structure mass is shown in Fig. 2. Figure 3 is a log-log plot of linear density $S = M/h$ (the inverse of the slope of the line in Fig. 2), as a function of Bond number. The central portion of this plot shows that the linear density $S = M/h$ scales as $S = A|\mathrm{Bo}|^{-\alpha}$, with $\alpha = 0.72 \pm 0.06$ and $A = 5.2 \pm 0.8$ [(pore volume)/(pore diameter)].

Simulations were carried out using a 3D cubic lattice, site invasion percolation model [5,6] and lattices of size $128 \times 128 \times 360$ (x,y,z) with periodic boundary conditions in the lateral (x,y) directions. In most simulations a single bubble or cluster was grown from a single site (injection point) at the center of the (x,y) substrate. The invasion threshold at the ith site was given by $T_i = f(r_i) + gz_i$, where r_i is a random number uniformly distributed over the range $0 < r_i < 1$ and g (the threshold gradient) is a constant. In most cases a uniform distribution of thresholds [$f(r) = r$] was used but similar scaling behavior was found for other (continuous) threshold distributions. Trapping [5] was not included in the simulations since in 3D the trapping probability is vanishingly small except for very small volumes. In order to reduce statistical uncertainties results from a large number of simulations (typically 100–1000 depending on the gradient g) were averaged. Each simulation was continued until the displacement pattern reached the upper ($z \simeq 360$) boundary and the linear density of the displaced volume was measured in a length interval (measured in the z direction) well removed from the upper and lower edges of the lattice. A detailed description of these simulations will be given elsewhere [13].

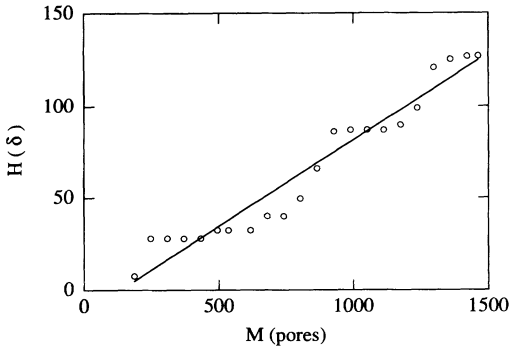

FIG. 2. Height of structure formed by the invading fluid during fluid migration in a transparent 3D porous medium as a function of structure mass. The height is given in terms of the grain size, and the mass in number of filled pore volumes. The structure shown in Fig. 1(a) is taken from this run.

Despite the complexities associated with any fluid-fluid

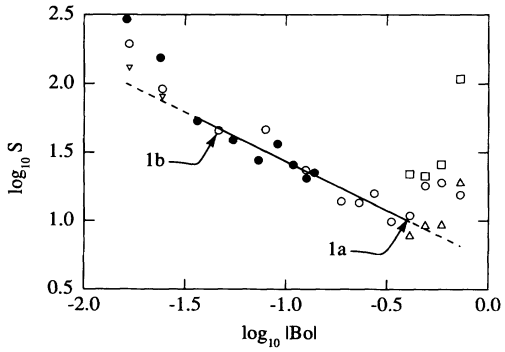

FIG. 3. The mass per unit length S as a function of Bond number $|\mathrm{Bo}|$ for the different 3D experiments. The straight line has a slope of 0.72. Points corresponding to the structures in Figs. 1(a) and 1(b) are indicated by arrows. Open symbols correspond to downward migration, solid to upward. Injection rates were 0.2 (△), 2 (●,○), 5 (▽), and 20 (□) ml/h.

displacement process the simple invasion percolation model provides a surprisingly accurate representation of our experiments. The displacement patterns generated in experiments and in simulations are qualitatively very similar. In both cases the linear density S has an algebraic dependence on the Bond number $|\mathrm{Bo}|$ with an effective exponent of $a=0.72\pm0.06$ from the experiments and $a=0.69\pm0.01$ from the simulations. For both the simulations and experiments the displacement pattern can be described in terms of a chain of blobs (with a characteristic size ξ) that form a directed random walk. The internal structure of the blobs is like that of an invasion percolation cluster with a fractal dimension $D\simeq2.50$. Such a chain of blobs has a mass that is proportional to its vertical length, i.e., it has a linear density that scales as $S\sim\xi^{D-1}$. The theoretical arguments used by Wilkinson [6] can be used to obtain the relationship $\xi\sim|\mathrm{Bo}|^{-\nu/(\nu+1)}$ between the length ξ and the Bond number (as discussed in Ref. [7] and in more detail in Ref. [13]). Here ν is the percolation correlation length exponent with a value of about [14] 0.88. A value $a=(D-1)\nu/(\nu+1)\simeq0.70$ therefore is predicted, in good agreement with our experiments and simulation results.

In the experiments the range over which we found power-law behavior was limited by effects specific to our physical system. Separate mechanisms dominated at high and low $|\mathrm{Bo}|$ numbers, giving rise to deviations from a pure invasion percolation growth. At low $|\mathrm{Bo}|$ numbers (the left-hand side of Fig. 3) the driving force (due to the density difference) was low, and capillary forces dominated. Under these conditions the process is susceptible to small changes in wetting properties or interfacial tension, caused by contaminations, dye molecules, or fluid absorption in the grains. In capillary rise experiments with these low $|\mathrm{Bo}|$ number fluids in Röhm XT 10/4 Plexi tubes we found a pronounced scatter in heights and poor reproducibility. The fact that the leftmost point in Fig. 3 corresponds to a capillary rise height $h\simeq250$ mm in a Plexi tube with radius $r=2$ mm demonstrates that capillary forces dominate over gravity forces in this regime. For increased injection rate the deviations were reduced. In attempts to run significantly slower experiments (not shown in Fig. 3) even higher values for the linear density S were indicated. This suggests that time-dependent processes influenced the growth.

The deviations at high $|\mathrm{Bo}|$ values (the right-hand side of Fig. 3) are attributed to viscous pressure gradients in the invading fluid. We did observe additional growth (higher values for the linear mass density S) and branching, which were expected effects of a viscous pressure gradient. We increased $|\mathrm{Bo}|$ by increasing the sugar content of the injected water. Thus we also increased the viscosity of the invading fluid (by a large factor in the high $|\mathrm{Bo}|$ number regime). Therefore the capillary number (ratio of viscous to capillary forces $\mathrm{Ca}=\mu_i u/\gamma$, where μ_i is the viscosity of the invading fluid and u the velocity of the structure tip) increased with $|\mathrm{Bo}|$ number. The increase in Ca was due to increases in both the viscosity μ_i and the velocity u (since the structures become thinner at higher $|\mathrm{Bo}|$ values). Under the standard conditions for our experiments (indicated by open circles in Fig. 3) substantial deviations from power-law behavior were found at the largest $|\mathrm{Bo}|$ values where $\mathrm{Ca}\geq10^{-5}$. These deviations increased with the injection rate and could be reduced by lowering it. We found in experiments at low rate (indicated by $\triangle$ in Fig. 3) that the onset of growth dominated by viscous effects again occurred at $\mathrm{Ca}\simeq10^{-5}$.

At the pore level we have observed a number of interesting dynamical phenomena. One manifestation of the complex dynamics of this growth process was the structure of $h(M)$ (see Fig. 2) and the steplike motion of the displacement structure tip. In connection with these bursts [15] the structure sometimes "snapped off" and disconnected parts could move independently some distance upwards. Further snapoffs diminished the length of the moving, disconnected parts until they were stuck in the matrix. The uppermost point would then move only after reconnection from the main structure (fluid was slowly injected at the bottom point). We also observed that a disconnected blob could withdraw fluid from portions of its lower parts on moving upwards; see Fig. 4. The noise in $h(M)$ was reflected as a substantial scatter of the data points in Fig. 3.

The experimental structures were driven, in the sense that the time needed for relaxation was longer than the time the experiment lasted. The relaxation involved (at high $|\mathrm{Bo}|$ values) a very slow flow along the string (no injection) until only a chain of disconnected blobs remained, as a skeleton of the structure. In some cases we observed that the blobs were connected by long threads, much thinner than the pore width, during the late stages of this process. The relaxed structure, the chain of blobs,

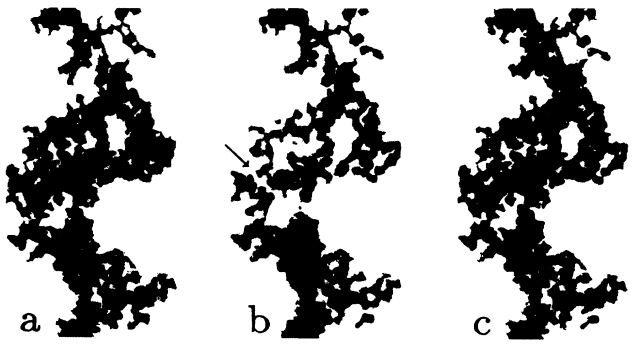

FIG. 4. Detail of a migration structure at three different times [(a)–(c)]. Portions of the structure [in (b)] above snapoff (disconnection) points (one of which is indicated by an arrow) were drained. Not all of the previously occupied pores were entered by the new invading fluid arriving from below [compare (c) to (a)]. The injection rate for this experiment was 2 ml/h, $\mathrm{Bo}\simeq-0.13$, and the time intervals were 1535 sec [(a) to (b)] and 1447 sec [(b) to (c)].

obtainable also in an experiment with much lower injection rate, is a subject of further study.

Many questions remain to be answered concerning the geometry, physical mechanisms, and dynamics of gravity-driven invasion percolation. A further study of the dynamics will offer opportunities for comparison between experiments and simulations and therefore for refinement of the numerical model. The experimental systems we have were large, of the order 10^6 grains. However, still larger systems will be necessary to study dynamical effects quantitatively. We believe that it should be possible to extend the range of Bond numbers for which S depends algebraically on $|\mathrm{Bo}|$ by using different materials. However, the selection of matrix material and fluids is strongly constrained by the large quantities needed and the requirements of the visualization technique.

We thank C. Hermanrud at STATOIL for pointing out the relevance of this process to secondary oil migration. We gratefully acknowledge support by (project B-2) VISTA, research cooperation between the Norwegian Academy of Science and Letters and Den norske stats oljeselskap a.s. (STATOIL) and by NAVF, the Norwegian Research Council for Science and the Humanities.

[1] R. Lenormand, E. Touboul, and C. Zarcone, J. Fluid Mech. **189**, 165 (1988); R. Lenormand and C. Zarcone, Physicochem. Hydrodyn. **6**, 497 (1985).

[2] M. M. Mandelbrot, *The Fractal Geometry of Nature* (Freeman, New York, 1982).

[3] J. Feder, *Fractals* (Plenum, New York, 1988).

[4] P. Meakin, in *Phase Transitions and Critical Phenomena*, edited by C. Domb and J. L. Lebowitz (Academic, New York, 1987), p. 336; P. Meakin, Rev. Geophys. **29**, 317 (1991).

[5] D. Wilkinson and J. F. Willemsen, J. Phys. A **16**, 3365 (1983).

[6] D. Wilkinson, Phys. Rev. A **30**, 520 (1984); **34**, 1380 (1986).

[7] A. Birovljev, L. Furuberg, J. Feder, T. Jøssang, K. J. Måløy, and A. Aharony, Phys. Rev. Lett. **67**, 584 (1991).

[8] E. Clément, C. Baudet, and J. P. Hulin, J. Phys. (Paris), Lett. **46**, L1163 (1985); E. Clément, C. Baudet, E. Guyon, and J. P. Hulin, J. Phys. D **20**, 608 (1987); J. P. Hulin, E. Clément, C. Baudet, J. F. Gouyet, and M. Rosso, Phys. Rev. Lett. **61**, 333 (1988).

[9] J.-D. Chen, M. M. Dias, S. Patz, and L. M. Schwartz, Phys. Rev. Lett. **61**, 1489 (1988).

[10] H. Dembicki and M. J. Anderson, Am. Assoc. Petrol. Geol. Bull. **73**, 1018 (1989).

[11] R. J. Glass, J.-Y. Parlange, and T. S. Steenhuis, Water Resour. Res. **27**, 1947 (1991), and references therein.

[12] A. W. Adamson, *Physical Chemistry of Surfaces* (Wiley, New York, 1976).

[13] P. Meakin, J. Feder, V. Frette, and T. Jøssang (to be published).

[14] D. Stauffer, *Introduction to Percolation Theory* (Taylor & Francis, London, 1985).

[15] L. Furuberg, J. Feder, A. Aharony, and T. Jøssang, Phys. Rev. Lett. **61**, 2117 (1988).